

infinitesimal spacetime volume around x . The real and imaginary parts of v_n correspond to $\cos(n\varphi)$ and $\sin(n\varphi)$ terms. The final observable anisotropy v_n is the weighted average

$$v_n(p_T; y) = \frac{\int d^4x S_0(x; p_T; y) v_n(x; p_T; y)}{\int d^4x S_0(x; p_T; y)}; \quad (2)$$

which is always real due to reflection symmetry across the collision plane $\varphi \rightarrow \varphi + \pi$ (for spherically symmetric nuclei). In addition, for a symmetric collision system, all odd v_n vanish at midrapidity $y = 0$ due to $\varphi \rightarrow \varphi + \pi$ symmetry.

In the following rapidity arguments will be often suppressed for brevity.

Momentum anisotropies from ideal hydrodynamics. Two main assumptions in approaches based on ideal hydrodynamics are local kinetic equilibrium and sudden freezeout on a 3D spacetime hypersurface. In such a case

$$S(x; p) = p \cdot (x) \cdot (x - x_0) f(x; p) \quad (3)$$

where (x) is the normalized normal vector of the hypersurface, while x_0 is an arbitrary point on the hypersurface [31], and

$$f_{th}(x; p) = \frac{g}{(2\pi)^3} e^{[p \cdot (x) - (x) \cdot T(x)] + a_s} \quad (4)$$

where g is the degeneracy factor, and $a_s = -1, 1$, or 0 respectively for bosons, fermions, or Boltzmann statistics. T , μ , and u are the local temperature, chemical potential, and flow velocity.

Momentum anisotropies have two sources, the hypersurface ($p \cdot (x)$) and the flow profile ($p \cdot u$). For hypersurfaces typically assumed in analytic studies, such as constant time or constant $t^2 - z^2$ hypersurfaces, $p \cdot (x)$ is independent of φ . Therefore, for simplicity we focus here on anisotropies due to the flow field only. Note, in general, φ dependence can appear even for azimuthally symmetric hypersurfaces [25].

The anisotropy coefficients in general depend on the particle species, mainly because of the difference in mass. Statistics and the chemical potentials only play a role at very low $m_T = \sqrt{m^2 + p_T^2}$; T . (At freezeout at RHIC, $T \approx 100 - 130$ MeV, while m increases from 80 MeV for pions to 350 MeV for heavy particles [4].)

To demonstrate the mass dependence, consider not very low momenta, so that Boltzmann statistics is applicable. The flow field can be characterized by a local transverse and longitudinal rapidity component, $v_T(x) = v_T \sqrt{\cos^2 \varphi + \sin^2 \varphi}$ and $\tilde{y}(x)$, as $u(x) = (ch\tilde{y}; v_T; sh\tilde{y}) = \frac{1}{\sqrt{1-v_T^2}} (ch\tilde{y}; v_T; sh\tilde{y})$. It is simple to show that

$$v_n(x; p_T; y) = e^{in\varphi(x)} \frac{I_n(sh\tilde{y}_T(x) p_T = T(x))}{I_0(sh\tilde{y}_T(x) p_T = T(x))}; \quad (5)$$

where $sh\tilde{y}_T = \frac{p_T}{m} \frac{1}{\sqrt{1-v_T^2}}$ and I_n are the modified Bessel functions. Remarkably, the local anisotropy depends only on p_T , and therefore is the same for all particles and rapidities. Note, at low p_T ,

$$j_n \approx (sh\tilde{y}_T p_T = 2T)^n = n! / p_T^n; \quad (6)$$

as dictated by general analyticity arguments [26], while at high p_T , $j_n \approx 1 - \text{const} \cdot T/p_T$.

The coordinate-averaged flow coefficients (2), on the other hand, in general decrease in magnitude with particle mass. This follows from the properties of the weight S_0 , which via (3) corresponds to the distribution

$$f_0 = \exp \left[\frac{m_T ch(\tilde{y} - \tilde{y}(x)) ch\tilde{y}_T(x)}{T(x)} - I_0 \frac{p_T sh\tilde{y}_T(x)}{T(x)} \right]$$

While j_n monotonically increases with the radial flow v_T , the only mass dependent part in f_0 , the exponential, decreases with v_T . The decrease is sharper for larger mass. Therefore for heavier particles, smaller v_n values get preferred. Though this argument ignores the x -dependence of the cosine term from the exponential in (5), which in principle could reverse the rise of $Re v_n$ with v_T and therefore affect the mass dependence pattern, the general trend prevails in practice.

For more details of the derivations in the case of $Re v_2$, see [25], for example.

Anisotropic flow from quark coalescence. In the quark coalescence approach, constituent quarks/antiquarks that are close in phase space can combine to form hadrons. Assuming coalescence occurs on a 3D spacetime hypersurface, the hadron binding energies are small, and coalescence is a relatively rare process [16, 17], the invariant hadron momentum distribution can be expressed [17, 18, 19, 27] in terms of the constituent phase space distributions and the hadron Wigner functions.

Ignoring variations of phase space distributions on length and momentum scales corresponding to a typical hadron (≈ 1 fm and ≈ 200 MeV), the phase space distributions of mesons and baryons created via $q + \bar{q} \rightarrow M$ and $q + q + \bar{q} \rightarrow B$ can be written as

$$f_B(x; p) = \frac{(2\pi)^3 g_B}{g^3} f(x; p) f(x; p) f(x; p) \\ f_M(x; p) = \frac{(2\pi)^6 g_M}{g^3} f(x; p) f(x; p) f(x; p); \quad (7)$$

Here g_p is the degeneracy of the particle (spin and color), while $p_i = p$. Because constituents are comoving, $p \approx p_i$ and the hadron momentum is shared roughly in proportion to constituent mass [17]. For hadrons composed of u, d , and s quarks, the sharing is approximately equal because of the relatively small difference between $m_{u,d} \approx 0.3$ GeV and $m_s \approx 0.5$ GeV. On the other hand, in hadrons that also contain a heavy quark, e.g., D mesons or the Λ_c , the heavy quark carries most of the momentum.

A direct implication of (7) is

$$\begin{aligned} v_{n;B}(\mathbf{x};p_T) &= \sum_{i=1}^X v_{n,i}(\mathbf{x};p_{T,i}) + v_{n;B}(\mathbf{x};p_T) \\ v_{n;M}(\mathbf{x};p_T) &= \sum_{i=1}^X v_{n,i}(\mathbf{x};p_{T,i}) + v_{n;M}(\mathbf{x};p_T); \end{aligned} \quad (8)$$

where to leading order in $v_{n,i}$, the corrections $v_{n;M}$ and $v_{n;B}$ are

$$v_n = \sum_{i \neq j; k=1}^X v_{n+k,i} v_{k;j} + \sum_{i < j; k=1}^X v_{n-k,i} v_{k;j} + O(\bar{v}; v_i^3) \quad (9)$$

with arguments identical to those in (8) dropped for brevity. Thus, if the corrections are small, v_n is additive, and in the absence of quark flavor dependence scales with quark number [15, 16].

Assuming, as for example in [16], that the spatial and momentum dependence of phasespace distributions factorize, the local v_n coefficients are the same everywhere and therefore the scaling carries over to the observable spacetime averages v_n . In this case, the local v_n must of course be real, and at RHIC the odd ones must vanish at midrapidity. The neglect of the correction terms v_2 for elliptic flow is then justified because the data show $v_6 \approx v_4 \approx v_2 \approx 1$.

On the other hand, the scaling does not hold for arbitrary distributions. For example, for thermal (Boltzmann) constituent phasespace distributions, coalescence (7) gives thermal hadron distributions because, for the weak bound states assumed, $m_M \approx m + m$, $m_B \approx m + m + m$ [27]. Therefore, anisotropies are the same as from hydrodynamics, i.e., depend on the hadron mass. This also follows from a direct calculation. For mesons, the kernel is $f_0 \otimes f_0; f_0; [1 + \sum_{n=1}^P (v_n; v_n; + c\mathbf{x})]$, which is identical to the hydrodynamic one with $m = m_M$. The exponential part is the same because $p_T = p_{T_1} + p_{T_2}$, momenta are shared such that $m_T \approx m_{T_1} + m_{T_2}$, and therefore also $y \approx y_1 \approx y_2$. The rest of the kernel and all meson flow anisotropies also agree, as can be shown using the exact flow addition formula

$$\begin{aligned} v_{n;M} &= \frac{\sum_{i=1}^P v_{n,i} + \sum_{k=1}^P (v_{n+k}; v_k; + c\mathbf{x}) + \sum_{k=1}^P v_{n-k}; v_k;}{1 + \sum_{k=1}^P (v_k; v_k; + c\mathbf{x})} \end{aligned} \quad (10)$$

and the Bessel function addition theorem. The direct proof for baryons is analogous but more involved.

Thus, for thermal constituent distributions, momentum anisotropies from quark coalescence depend on mass, and not quark number. There is an intuitive way to see

why this must be so. In the frame where the flow velocity is zero, the momentum distribution is isotropic for all constituents. Therefore, in that frame all v_n vanish, and hence (8) gives no hadron anisotropies. The only source of anisotropy then is the Lorentz boost back to the laboratory frame, which depends only on the particle mass, momentum, and the boost velocity. This is also true even if hydrodynamics breaks down, as long as distributions are of the form $f(\mathbf{x};\mathbf{p}) = g(\mathbf{p} \cdot \mathbf{u}(\mathbf{x});\mathbf{x})$. Quark number scaling can emerge only if, in any frame, at least one of the constituent distributions is anisotropic.

In the thermal case, quark number scaling is violated because the nonlinear terms (9) are important. Consider for example v_2 , at low p_T so that (6) is justified. To leading $O(p_T^2)$ order, both the linear and the $v_1 v_1$ terms contribute. In fact the latter give as much as half the meson v_2 , and two-thirds for baryons. For higher-order flow coefficients, all $v_{n-k} v_k$ terms contribute at leading order in p_T .

Therefore, one class of freezeout distributions (besides uniform local anisotropy v_n) for which the observable v_n scales with quark number is when

$$v_n \propto v_{n-k} v_k \quad (11)$$

in the spacetime region where most particles are emitted from. In this case, there is (approximate) scaling locally and, because the formula is linear, scaling is preserved upon averaging. Note, a small amount of other anisotropies, for example $v_1 \propto v_2^{3/2}$ besides a pure v_2 , can even help compensate the denominator in (10), which otherwise tends to reduce the flow relative to the scaling expectation.

The scaling may also hold even if the nonlinear terms are important. However, that requires a high degree of fortuitous cancellations at RHIC, as illustrated in Fig. 1. Results from the covariant parton transport model MPC [21, 22, 29] are shown for Au + Au at $\sqrt{s_{NN}} = 200$ GeV with $b = 8$ fm, from a calculation identical to the one in [21] with a gluon-gluon cross section $\sigma_{gg} = 10$ mb. In the left panel local constituent quark anisotropies up to fourth order are plotted as a function of transverse momentum, averaged over the first quadrant of the transverse plane ($0 < \phi_x < \pi/2$, where $\mathbf{x}_T = x_T (\cos \phi_x; \sin \phi_x)$). Coefficients that vanish upon a full spacetime average due to symmetry, in particular v_1 and $\text{Im } v_2$, are surprisingly large. Therefore, (11) does not hold and, for example, the denominator in (10) exceeds 2 above $p_{T,i} > 1$ GeV.

The origin of these large anisotropies is shown in the right panel of Fig. 1, where we plot the distributions at midrapidity for $2 < p_T < 3$ GeV, averaged over four wedges in the transverse plane $\phi_x \in [k\pi/8; (k+1)\pi/8]$, with $k = 0; 1; 2; 3$. Instead of smooth harmonic modulations over a uniform background, the distributions are strongly peaked because high- p_T particles can only escape from a surface layer of the reaction region. In this

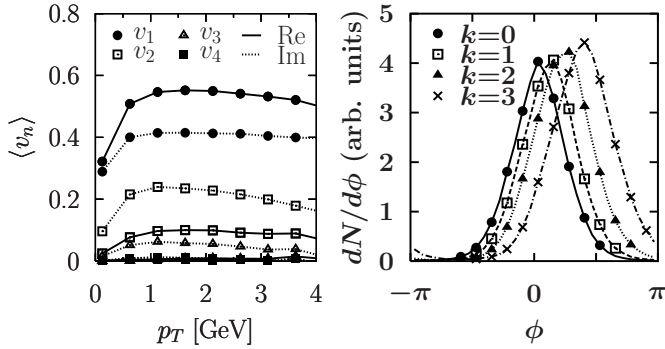


FIG. 1: Results from MPC [22, 29] for Au + Au at $p_{\text{SNN}} = 200$ GeV with $b = 8$ fm. Left: local constituent quark anisotropies at midrapidity as a function of p_T , averaged over the first quadrant of the transverse plane. Right: distributions at midrapidity for $2 < p_T < 3$ GeV, averaged over four wedges in the transverse plane $\times 2$ [$k=8$; $(k+1)=8$], with $k = 0 \dots 3$.

case, anisotropies from coalescence change their character completely. Consider, for simplicity, Gaussian constituent distributions around an azimuthal direction ϕ_0 , $S_i(\mathbf{x}; p_T; y) = C_i(\mathbf{x}; p_T; y) \exp[-(\phi - \phi_0)^2 / (2\sigma_i^2)]$. For not too wide $\sigma_i < 2\pi / (n+1)$, the constituent and hadron anisotropies

$$v_{n,i} \sim e^{in\phi_0} e^{-n^2 \sigma_i^2 / 2}; \quad v_{n,h} \sim e^{in\phi_0} e^{-n^2 \sigma_h^2 / 2}; \quad (12)$$

scale as $(\text{const})^{-n^2}$. This is very different from both (5) and (11). For example, if all constituents have the same width σ , we have

$$j_{n,B}(3p_T) j'_{n,q}(p_T) \neq j_{n,M}(2p_T) j'_{n,q}(p_T);$$

which is a complete reversal of the constituent-meson-baryon flow ordering $v_{n,B}(3p_T) = 3v_{n,q}(p_T)$, $v_{n,M}(2p_T) = 2v_{n,q}(p_T)$ from linear scaling (8).

The observable averages $\langle v_n \rangle$ are, of course, determined by the interplay between variations in the local emission angle, the width, and constituent density. It is quite remarkable that the end result in a dynamical coalescence approach [21] is only a modest 20% and 30% reduction of pion and proton elliptic flow at RHIC relative to quark number scaling.

The above results underscore the importance of local momentum anisotropies in hadronization via quark coalescence. Flow addition formulas apply locally, even though only spacetime averages of the final anisotropies can be observed. Odd-order $\langle v_n \rangle$ and the sine terms play a major role, even at midrapidity. These terms have been ignored in analytic studies so far [16, 30] but are naturally incorporated in a dynamical approach [21].

Acknowledgments. Helpful discussions with E. Shuryak and U. Heinz are gratefully acknowledged. This work was supported by DOE grant DE-FG 02-01ER 41190.

- [1] For reviews see, e.g., J. Ollitrault, Nucl. Phys. A 638, 195 (1998); A.M. Poskanzer, nucl-ex/0110013; or S.A. Voloshin, Nucl. Phys. A 715, 379 (2003).
- [2] C. Adler et al. [STAR Collaboration], Phys. Rev. Lett. 90, 032301 (2003); K. Filimonov [STAR Collaboration], Nucl. Phys. A 715, 737 (2003).
- [3] K. Adcox et al. [PHENIX Collaboration], Phys. Rev. Lett. 89, 212301 (2002); N.N. Ajitanand [PHENIX Collaboration], Nucl. Phys. A 715, 765 (2003).
- [4] B. B. Back et al. [Phobos Collaboration], nucl-ex/0407012.
- [5] C. Adler et al. [STAR Collaboration], Phys. Rev. Lett. 87, 182301 (2001).
- [6] S. S. Adler et al. [PHENIX Collaboration], Phys. Rev. Lett. 91, 182301 (2003).
- [7] M. Kaneta [PHENIX Collaboration], nucl-ex/0404014.
- [8] J. Adams et al. [STAR Collaboration], Phys. Rev. Lett. 92, 052302 (2004); C. Adler et al. [STAR Collaboration], Phys. Rev. Lett. 89, 132301 (2002).
- [9] J. Castillo [STAR Collaboration], nucl-ex/0403027.
- [10] J. Ollitrault, Phys. Rev. D 46, 229 (1992).
- [11] P. F. Kolb, J. Sollfrank and U. Heinz, Phys. Rev. C 62, 054909 (2000).
- [12] P. Huovinen et al., Phys. Lett. B 503, 58 (2001).
- [13] D. Teaney, J. Lauret and E. V. Shuryak, nucl-th/0110037.
- [14] T. Hirano and K. T. Suda, Phys. Rev. C 66, 054905 (2002); T. Hirano, private communication.
- [15] S.A. Voloshin, Nucl. Phys. A 715 (2003) 379.
- [16] D. Molnar and S.A. Voloshin, Phys. Rev. Lett. 91, 092301 (2003).
- [17] Z. W. Lin and D. Molnar, Phys. Rev. C 68 (2003) 044901.
- [18] R. J. Fries et al., Phys. Rev. Lett. 90, 202303 (2003); R. J. Fries et al., Phys. Rev. C 68, 044902 (2003).
- [19] V. Greco, C. M. Ko and P. Levai, Phys. Rev. Lett. 90, 202302 (2003); Phys. Rev. C 68, 034904 (2003).
- [20] R. C. Hwa and C. B. Yang, Phys. Rev. C 66, 025205 (2002); ibid. 67, 034902 (2003).
- [21] D. Molnar, nucl-th/0406066; J. Phys. G 30, S1239 (2004).
- [22] D. Molnar and M. Gyulassy, Nucl. Phys. A 697, 495 (2002), A 703, 893(E) (2002); ibid. A 698, 379 (2002).
- [23] D. Teaney, Nucl. Phys. A 715, 817 (2003); Phys. Rev. C 68, 034913 (2003).
- [24] V. Greco and C. M. Ko, nucl-th/0402020.
- [25] U. Heinz and S. M. H. Wong, Phys. Rev. C 66, 014907 (2002).
- [26] P. Danielewicz, Phys. Rev. C 51, 716 (1995).
- [27] C. B. Dover et al., Phys. Rev. C 44, 1636 (1991). R. Scheibl and U. Heinz, Phys. Rev. C 59, 1585 (1999).
- [28] J. Adams et al. [STAR Collaboration], Phys. Rev. Lett. 92, 062301 (2004).
- [29] D. Molnar, MPC 1.6.7. This parton cascade code is available at <http://nt3.phys.columbia.edu/people/molnar/>.
- [30] P. F. Kolb et al., Phys. Rev. C 69, 051901 (2004).
- [31] Note, \times is a generalized time, and $\hat{\mathbf{x}} \cdot \mathbf{p} \hat{\mathbf{x}}(\mathbf{x}) f$.